12556–12565 *Nucleic Acids Research, 2020, Vol. 48, No. 22* *Published online 3 December 2020*
doi: 10.1093/nar/gkaa1109

Structural properties and anticoagulant/cytotoxic activities of heterochiral enantiomeric thrombin binding aptamer (TBA) derivatives

Antonella Virgilio[1,†], Veronica Esposito[1,†], Annalisa Pecoraro[1], Annapina Russo[1], Valentina Vellecco[1], Antonietta Pepe[2], Mariarosaria Bucci[1], Giulia Russo[1] and Aldo Galeone[1,*]

[1]Department of Pharmacy, University of Naples Federico II, Via Domenico Montesano 49, 80131 Naples, Italy and [2]Department of Sciences, University of Basilicata, Viale dell'Ateneo Lucano 10, I-85100 Potenza, Italy

Received July 15, 2020; Revised October 09, 2020; Editorial Decision October 27, 2020; Accepted November 30, 2020

ABSTRACT

The thrombin binding aptamer (TBA) possesses promising antiproliferative properties. However, its development as an anticancer agent is drastically impaired by its concomitant anticoagulant activity. Therefore, suitable chemical modifications in the TBA sequence would be required in order to preserve its antiproliferative over anticoagulant activity. In this paper, we report structural investigations, based on circular dichroism (CD) and nuclear magnetic resonance spectroscopy (NMR), and biological evaluation of four pairs of enantiomeric heterochiral TBA analogues. The four TBA derivatives of the D-series are composed by D-residues except for one L-thymidine in the small TT loops, while their four enantiomers are composed by L-residues except for one D-thymidine in the same TT loop region. Apart from the left-handedness for the L-series TBA derivatives, CD and NMR measurements have shown that all TBA analogues are able to adopt the antiparallel, monomolecular, 'chair-like' G-quadruplex structure characteristic of the natural D-TBA. However, although all eight TBA derivatives are endowed with remarkable cytotoxic activities against colon and lung cancer cell lines, only TBA derivatives of the L-series show no anticoagulant activity and are considerably resistant in biological environments.

INTRODUCTION

Among the secondary conformations of DNA and RNA, the G-quadruplex structures (G4) represent a very current topic, as they are involved in many research fields ranging from molecular biology and genetics to nanotechnology. The interest toward nucleic acid sequences adopting these secondary structures is further increased by their employment also in diagnostics and pharmaceutics, considering that they have proven to represent both promising pharmacological targets for druggable small molecules (1) and potential pharmacological agents themselves (2). Particularly, several DNA and RNA aptamers (ligands endowed with outstanding affinity and specificity toward a given target of diagnostic or therapeutic interest) adopt K^+ ion dependent G-quadruplex structures, which are among the most stable nucleic acid conformations (3).

From a therapeutic point of view, the antiproliferative and anticancer G-quadruplex aptamers are particularly appealing, as documented by the advanced status of development as drug of one of them, namely the 26-mer AS1411 (4). Interestingly, this aptamer shares the antiproliferative activity against HeLa cervical carcinoma cells with other G-quadruplex forming sequences (5), thus suggesting that this biological property may be a general aspect of some G-rich ODNs (6). Among these, the 15-mer TBA (thrombin binding aptamer, $G_2T_2G_2TGTG_2T_2G_2$) has recently raised great interest as a potential anticancer agent, due to its noteworthy antiproliferative activity, relatively reduced size and, contrarily to the polymorphic AS1411, its ability to fold in a well-defined G-quadruplex structure (antiparallel orientation of the G-tracts and presence of two stacked G-tetrads connected through one large TGT loop and two small TT loops) (Figure 1) (7). Formerly developed as anticoagulant aptamer, the TBA has been undergone to many chemical modifications aimed at improving its biological activity, thermal stability and resistance in biological environments (8,9). However, in view of a future development of TBA derivatives as anticancer agents, most of the recent modifications have been addressed to preserve the antiproliferative activity to the detriment of the anticoagulant one (to be considered as a side effect) and im-

*To whom correspondence should be addressed. Tel. +39 081678542; Email: galeone@unina.it
†The authors wish it to be known that, in their opinion, the first two authors should be regarded as Joint First Authors.

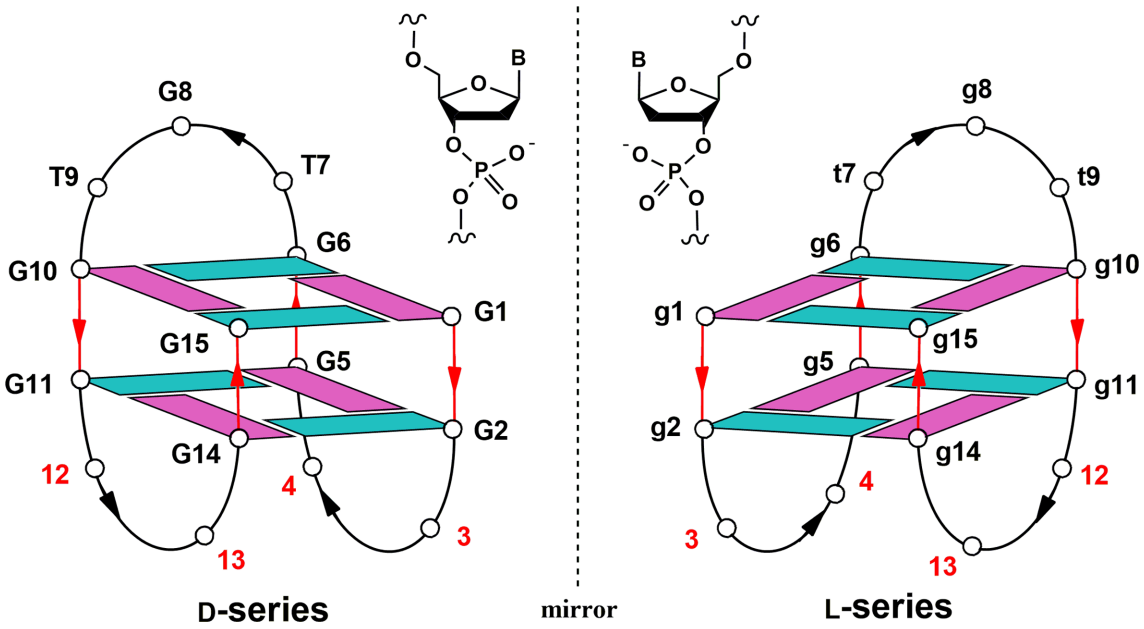

Figure 1. G-quadruplex structures adopted by the enantiomeric ODNs investigated (Table 1). The positions in which thymidines with opposite chirality to the rest of the sequence have been individually introduced are indicated in red. Upper and lower case letters indicate D-nucleotides and L-nucleotides, respectively. *Anti* and *syn* guanosines are indicated in green and purple, respectively.

prove the resistance to nucleases. For example, a derivative with a noteworthy antiproliferative activity against HeLa cervical carcinoma cells and no anticoagulant activity has been obtained by replacing thymidine in position 13 in one of the small loop with a dibenzyl linker (10). The incorporation of 4-thiouridine RNA and 4-thiouridine unlocked nucleic acid (UNA) residues in specific positions has been reported as a further TBA modification suitable to obtain similar effects on the same type of cells (11). Remarkably, while the introduction of a 5-hydroxymethyl-2′-deoxyuridine residue in position 9 (in large TGT loop) is able to improve the anticoagulant activity (12), the replacement of thymidines 4 or 13 (in small TT loops) with the same modified uridine results in TBA derivatives possessing an antiproliferative activity against lung cancer (Calu-6) and colorectal cancer cells (HCT 116$^{p53-/-}$) similar to TBA and a negligible residual anticoagulant activity (13). As far as the backbone modifications are concerned, non-anticoagulant TBA derivatives endowed with antiproliferative properties against human lung carcinoma A549 cells have been obtained by introducing alkylated phosphorothioate ester bonds (14). Interestingly, also more drastic backbone modifications as, for example, the introduction of inversion of polarity sites, can afford derivatives with no anticoagulant properties but endowed with antiproliferative activity against Calu-6 and HCT 116$^{p53-/-}$ cells (15). However, it should be noted that, if antiproliferative TBA derivatives are intended to be used for therapeutic purposes, they have to be also stabilized against cleavage by endo- and exonucleases, ubiquitous in biological environments. Although straightforward modifications have been reported able to increase the nuclease resistance of certain anticoagulant TBA derivatives *in vitro* (16), some degree of biological instability remains for the antiproliferative TBA analogues described above, being mostly composed by natural occurring nucleotides.

In this frame, as in the case of the Spiegelmers (aptamers composed by L-nucleotides) (17), a rather innovative modification of TBA has concerned the introduction of L-residues (18,19) which, being mirror-image of natural occurring residues, are not recognized by the ubiquitous plasma nucleases. Recently, we have shown that the homochiral L-TBA and the heterochiral LQ1, formerly TBA-D13 (the last mostly composed by L-residues except for the thymidines in the small TT loops), are endowed with noteworthy antiproliferative activities against Calu-6 and HCT 116$^{p53-/-}$ cells, an outstanding stability to nucleases but no anticoagulant activity (20). In a following study, we investigated the molecular mechanisms of LQ1 activity and the structural and antiproliferative properties of two further heterochiral TBA derivatives (differing from LQ1 only by the small loop base-compositions), thus highlighting the critical importance of the small loops for the antiproliferative activity against Calu-6 and HCT 116$^{p53-/-}$ cells (21).

In the present paper, we have investigated the structural and biological properties of four pairs of enantiomeric heterochiral TBA analogues in which only one residue at a time having an opposite chirality to the rest of the sequence has been introduced into the TT loops (Table 1).

MATERIALS AND METHODS

Oligonucleotides synthesis and purification

Modified ODNs reported in Table 1 were synthesized by an ABI 394 DNA synthesizer using solid phase β-cyanoethyl phosphoramidite chemistry at 10 μmol scale. The modified 5′-dimethoxytrityl-β-L-deoxythymidine-3′-phosphoramidite monomer is commercially available

Table 1. Sequence and melting temperature (T_m) of the TBA derivatives investigated

Oligonucleotide	Sequence (5′-3′)[a]	handedness	T_m (°C) ± 1
D-TBA	GGTTGGTGTGGTTGG	Right	50[b]
D-TBA-L3	GGtTGGTGTGGTTGG	Right	49
D-TBA-L4	GGTtGGTGTGGTTGG	Right	48
D-TBA-L12	GGTTGGTGTGGtTGG	Right	50
D-TBA-L13	GGTTGGTGTGGTtGG	Right	49
L-TBA-D3	ggTtggtgtggttgg	Left	50
L-TBA-D4	ggtTggtgtggttgg	Left	48
L-TBA-D12	ggttggtgtggTtgg	Left	50
L-TBA-D13	ggttggtgtggtTgg	Left	49

[a]Upper and lower case letters indicate D-nucleotides and L-nucleotides, respectively. [b]Data from (9).

(ChemGenes). For all ODNs an universal support was used. The oligomers were detached from the support and deprotected by treatment with concentrated aqueous ammonia at 80°C overnight. The combined filtrates and washings were concentrated under reduced pressure, redissolved in H_2O, analyzed and purified by high-performance liquid chromatography on a Nucleogel SAX column (Macherey-Nagel, 1000-8/46), using buffer A: 20 mM NaH_2PO_4/Na_2HPO_4 aqueous solution (pH 7.0) containing 20% (v/v) CH_3CN and buffer B: 1 M NaCl, 20 mM NaH_2PO_4/Na_2HPO_4 aqueous solution (pH 7.0) containing 20% (v/v) CH_3CN; a linear gradient from 0 to 100% B for 45 min and flow rate 1 ml/min were used. The fractions of the oligomers were collected and successively desalted by Sep-pak cartridges (C-18). The isolated oligomers proved to be >98% pure by NMR.

Nuclear magnetic resonance

NMR samples were prepared at a concentration of about 1.5 mM, in 0.6 ml (H_2O/D_2O 9:1 v/v) buffer solution having 10 mM KH_2PO_4/K_2HPO4, 70 mM KCl and 0.2 mM EDTA (pH 7.0). All the samples were heated for 5–10 min at 90°C and slowly cooled (10–12 h) to room temperature. The solutions were equilibrated for several days at 4°C. The annealing process was assumed to be complete when ^{1}H-NMR spectra were superimposable on changing time. NMR spectra were recorded with Varian Unity INOVA 500 MHz spectrometer. 1D proton spectra of the sample in H_2O were recorded using pulsed-field gradient DPFGSE for H_2O suppression. ^{1}H-chemical shifts were referenced relative to external sodium 2,2-dimethyl-2-silapentane-5-sulfonate (DSS). Pulsed-field gradient DPFGSE sequence was used for NOESY (180 ms and 80 ms mixing times) and TOCSY (120 ms mixing time) experiments in H_2O. All experiments were recorded using STATES-TPPI procedure for quadrature detection. In all 2D experiments, the time domain data consisted of 2048 complex points in t2 and 400–512 fids in t1 dimension. A relaxation delay of 1.2 s was used for all experiments.

Circular dichroism

CD samples of modified oligonucleotides and their natural counterpart were prepared at a ODN concentration of 50 μM by using a potassium phosphate buffer (10 mM KH_2PO_4/K_2HPO_4, 70 mM KCl, pH 7.0) and submitted to the annealing procedure (heating at 90°C and slowly cooling at room temperature). CD spectra of all quadruplexes and CD melting/annealing curves were registered on a Jasco 715 CD spectrophotometer by taking the average of three scans. For the CD spectra, the wavelength was varied from 220 to 320 nm at 100 nm min^{-1} scan rate, and the spectra recorded with a response of 16 s, at 2.0 nm bandwidth and normalized by subtraction of the background scan with buffer. The temperature was kept constant at 20°C with a thermoelectrically controlled cell holder (Jasco PTC-348). CD melting/annealing curves were registered as a function of temperature (range: 20–90°C) for all quadruplexes at their maximum Cotton effect wavelengths. The CD data were recorded in a 0.1 cm pathlength cuvette with a scan rate of 0.5°C/min. The melting temperature (T_m) values provide the best fit of the experimental melting data.

Prothrombin time (PT) assay

PT assay was performed on human plasma. The assay was measured by using Koagulab MJ Coagulation system with a specific kit HemosIL RecombinPlasTin 2G (Instrumentation Laboratory, Milan, Italy). Briefly, this method relies on the high sensitivity of thromboplastin reagent based on recombinant human tissue factors. The addition of recombiplastin to the plasma, in presence of calcium ions, initiates the activation of extrinsic pathway that culminates with the conversion of fibrinogen into fibrin and, in turn, with a formation of a solid gel. In our experimental conditions, each ODN or vehicle was incubated with 100 μl of plasma at 37°C for 15 min and then 200 μl of the kit solution containing recombiplastin was added with the consequent activation of the extrinsic pathway. In particular, for the evaluation of PT at the concentration of 20 μM, 2 μl of the corresponding ODN solution (1 mM) or vehicle (phosphate buffer saline, PBS) was added to the apposite microtube. For the evaluation of PT at 2 μM, 2 μl of a diluted solution (0.1 mM ODN solution in PBS buffer) was added to the apposite microtube. The PT measurement was produced in triplicate and the average and the standard error values were calculated and expressed as seconds. The basal clotting time was evaluated by measuring the clotting time in presence of vehicle.

Cell cultures and treatments with the ODNs

Calu-6 and HCT 116$^{p53-/-}$ cell lines were cultured as previously reported (22). Treatments of cells were performed

replacing the culture medium with those containing ODNs at final concentration of 10 and 50 μM.

MTT assay

Calu-6 (23) and HCT $116^{p53-/-}$ cells (24) were seeded onto 96-well plates at density of 1×10^4 cells/well and treated with different ODNs at final concentration of 10 μM and 50 μM from 24 to 72 h. Then, cell viability was determined using the MTT assay as previously reported (25). A pool of three different sets of experiments each repeated in triplicate were performed. Error bars represent mean ± SEM from $n = 3$ biological replicates. Statistical comparisons were made as previously shown (26).

RT-qPCR

Total RNA was isolated from cells as previously described (27). RNA was first retrotranscribed using SensiFAST™ cDNA Synthesis kit (Bioline) and then quantitative PCR was carried out using SensiFAST SYBER® No-ROX kit. Primers for β-actin were used for loading control amplifications. Specific primer sets used for each gene are: GDA Forward (5′ to 3′) GCAACAATTCACACTGACTCATC; GDA Reverse (5′ to 3′) GTGTCACTATGGGCTTCACT C; β-actin Forward (5′ to 3′) CCAACCGCGAGAAGAT GA; β-actin Reverse (5′ to 3′) CCAGAGGCGTACAGGG ATAG. The comparative Ct method was used to calculate the relative abundance of the mRNA and compared with that of β-actin expression. Statistical analysis was performed as previously described (28).

Nuclease stability assay

Nuclease stability assay of modified ODNs was conducted in 10% fetal bovine serum (FBS) diluted with Dulbecco's modified Eagle's medium (DMEM) at 37°C and studied by CD analysis. Approximately 7 nmol of stock solution of each ODN (~1 O.D.U.) was evaporated to dryness under reduced pressure and then incubated with 250 μl 10% FBS at 37°C. The degradation patterns were analyzed by monitoring the CD signal decrease of each sample at 37°C, as a function of time. CD spectra at 0 and 24 h for TBA derivatives of the D-series, and at 0, 24, 48 and 72 h for TBA derivatives of the L-series were recorded at 37°C using a Jasco 715 spectrophotometer equipped with a Peltier temperature control system (Jasco, Tokyo, Japan). Data were collected from 240 to 320 nm with a 1 s response time and a 1 nm bandwidth using a 0.1 cm quartz cuvette. Each spectrum shown is corrected for the spectrum of the reaction medium (10% FBS in DMEM).

RESULTS AND DISCUSSION

Structural insight of the investigated sequences

The modified TBA sequences were firstly investigated by CD, in order to test their ability to adopt a G-quadruplex conformation similar to the natural one. ODNs composed mainly of D-nucleotides (D-series) showed CD profiles comparable among each other (Figure 2), apart from slight differences in intensity, and strictly similar to that of TBA, that

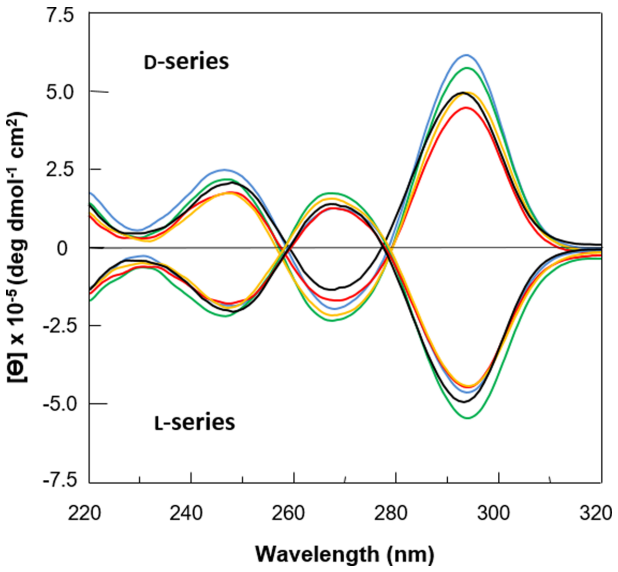

Figure 2. CD spectra at 20°C of D-TBA (black), D-TBA-L3 (blue), D-TBA-L4 (green), D-TBA-L12 (red), D-TBA-L13 (yellow) (D-series) and L-TBA (black), L-TBA-D3 (blue), L-TBA-D4 (green), L-TBA-D12 (red), L-TBA-D13 (yellow) (L-series) at 50 μM ODN strand concentration in a buffer solution 10 mM KH_2PO_4/K_2HPO_4, 70 mM KCl (pH 7).

is characterized by two positive bands around 247 and 294 nm, and a negative one around 266 nm. These data clearly suggest that the replacement of a single D-residue with one L in the small TT loops does not alter the ability to form the antiparallel 'chair-like' G-quadruplex structure typical of the unmodified aptamer. Instead, the comparison of the CD profiles of sequences composed mainly of L-nucleotides (L-series) with that of L-TBA (the mirror image of natural TBA) strongly suggested that they fold similarly to it and, apart handedness, to the TBA itself. CD melting measurements were also used to evaluate the thermal stability of the modified ODNs (Supplementary Figure S1). The well-defined sigmoidal CD heating profiles of TBA derivatives allowed us to measure the melting temperatures (T_m) (Table 1), recording values ranging from 48 to 50°C, strictly similar to that of their natural counterpart (50°C) (9). These data suggest that the single D/L substitutions into the small TT loops does not affect significantly the thermal stability of the G-quadruplex structures adopted. Furthermore, melting and annealing profiles of each TBA derivative are quite superimposable (Supplementary Figure S1), similarly to that of the original TBA.

The ability of all the derivatives to fold into a TBA-like antiparallel quadruplex was also assessed by NMR spectroscopy. The simple appearance of all ^{1}H-NMR spectra indicates that, in the conditions used here, the modified oligomers form mainly a single well-defined hydrogen-bonded conformation. In fact their one-dimensional ^{1}H-NMR spectra, (500 MHz, $T = 25$°C) (Figure 3 and Supplementary Figure S2) in the K^+ containing buffer utilized, showed principally the presence of eight signals in the region 11.5–12.5 ppm, attributable to imino protons involved in Hoogsteen hydrogen bonds of at least two G-quartets and, moreover, fifteen main signals in the aro-

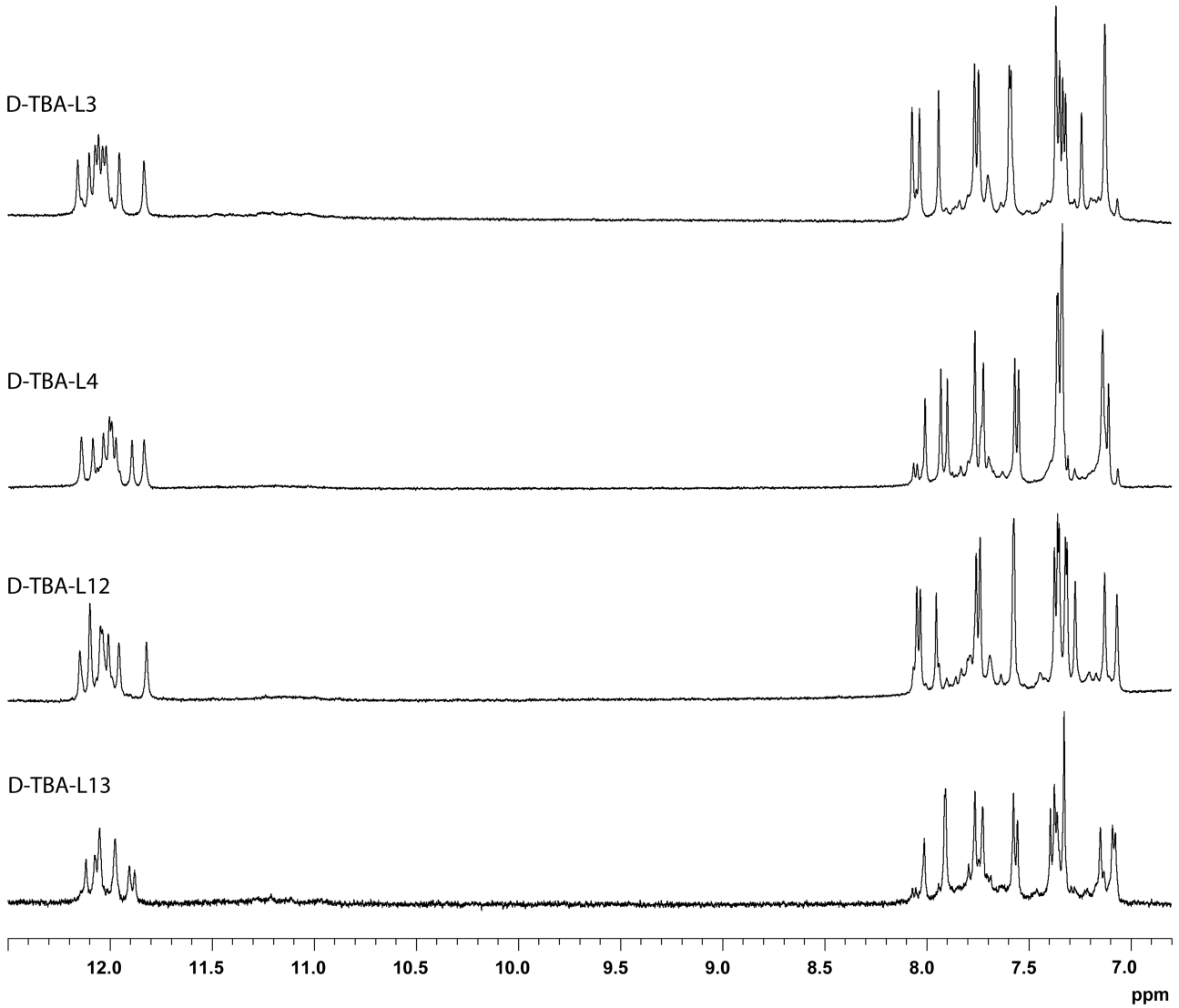

Figure 3. Imino and aromatic regions of the ^{1}H-NMR spectra of the D-series TBA derivatives (Table 1). See the main text and the Materials and Methods section for details.

matic region, (7.0–8.5 ppm), due to the presence of nine guanine H8 and of six thymine H6 singlets. As expected, the NMR profiles of the quadruplexes belonging to the two enantiomeric series are superimposable for each enantiomeric pair (Figure 3 and Supplementary Figure S2). For this reason, more detailed 2D-NMR investigations were carried out only for the ODNs belonging to the D-series of the enantiomeric TBA derivatives. A combination of the analysis of 2D NOESY (Supplementary Figures S3–S6) and TOCSY spectra (data not shown) allowed us to get the almost complete assignment (Supplementary Tables S1 and S2) of the non-exchangeable protons. The intensities of NOESY crosspeaks between the aromatic base proton and sugar H1′ resonances of the modified thrombin aptamers indicate that four Gs (G1, G5, G10 and G14) adopt *syn* glycosidic conformations, while five Gs (G2, G6, G8, G11 and G15) adopt *anti* conformations, where the H8 resonances of the *syn* Gs are upfield shifted with respect to those of the *anti* ones (29–31). All the thymidines, including the L ones, also show *anti* glycosidic conformations. Then, four *anti*-Gs (G2, G6, G11 and G15) have classical H8/H2′-H2″ sequential connectivities to 5′ neighboring *syn*-Gs (G1, G5, G10 and G14, respectively) indicating that the subunits G1-G2, G5-G6, G10-G11 and G14-G15 are involved in the formation of a four-stranded helical structure (underlined residues adopt a *syn* glycosidic conformation). In summary, as observed for the parent TBA, there are 5′-G*syn*G*anti*-3′ steps along each strand of the two quartets and, moreover, the entire pattern of NOEs observed for all cited Gs indicates that the backbone conformations of these tracts resemble those of the unmodified TBA possessing a right-handed helix structure. The alternation of *syn* and *anti* G residues within each strand suggests that, as for TBA, all four the modified oligomers fold into a monomolecular chair-like foldback G-quadruplex, characterized by two G tetrads. Two stretches of 5′-TT-3′, including an L-T residue at time, and one of 5′-TGT-3′ could also be identified on the basis of *anti–anti* connectivities. All the stretches of se-

quential connectivities were arranged using the information in long-range NOE connectivities. Similar to the case of the parent TBA, for all the samples, there is a number of NOE connectivities observed between residues not adjacent in sequence. In particular, there are NOE connectivities between H8 of G8 and H1′, H2′ and H2″ of G6 and between H1′ of T9 and H8 of G15, thus indicating that G8 and T9 residues in the TGT loop are near to the G1–G6–G10–G15 tetrad in all the four TBA analogues. NOEs are also present between H8 of G2 and methyl and H2″ and H1′of L-T4 and between H8 of G11 and methyl, H2′ and H2″ and H1′of T13 in the case of D-TBA-L4. Complementary information is provided by the NOEs from the methyl of L-T4 with H1′, H2′ and H2″ of G2 and from the methyl of T13 with H1′, H2′ and H2″ of G11. Correspondingly, as far as D-TBA-L13 is concerned, there are NOE connectivities between H8 of G2 and methyl, H2′ and H2″ of T4 and between methyl of L-T13 with H1′, H2′ and of G11. As regarding D-TBA-L3 and D-TBA-L12, in particular, NOEs are present between H8 of G2 and methyl, H2′ and H2″ of T4 and between H8 of G11 and methyl, H2′ and H2″ of T13. Corresponding information is provided by the NOEs from the methyl of T4 with H1′, H2′ and H2″ of G2 and from the methyl of T13 with H1′, H2′ and H2″ of G11. For all the samples, this collection of NOEs places the residues in position 4 and 13 close to the G2–G5–G11–G14 tetrad, even when an L-T residue was introduced. The whole of NMR data showed that, as strongly suggested by the CD experiments, these four modified aptamers adopt G-quadruplex structures strictly resembling the parent one.

Anticoagulant activity

In order to investigate the possible anticoagulant activity of the TBA derivatives containing the modified residues in positions 3, 4, 12 and 13, the four pairs of enantiomeric heterochiral TBA analogues were applied for PT assay. The results clearly showed that TBA derivatives mostly composed by L-nucleotides (L-series) are completely devoid of anticoagulant activity (Figure 4A). Conversely, the TBA derivatives mostly composed by natural D-nucleotides (D-series) preserve their anticoagulant activities to some extent. In details, at the lowest concentration (2 μM), all TBA derivatives belonging to the D-series showed a significant reduction of anticoagulant activity when compared to the original TBA, slightly more marked for D-TBA-L4 and D-TBA-L13 (Figure 4B). However, when the same compounds were tested at the highest concentration (20 μM), all the TBA derivatives of the D-series showed a significant anticoagulant profile, even though with a lesser extent compared to the original TBA (Figure 4C).

Cytotoxic activity

To explore the dose-dependent cellular response to the investigated ODNs, two concentrations (10 and 50 μM) of different TBA derivatives were tested for their ability to inhibit cell viability, in two different cancer cell lines. Specifically, HCT 116$^{p53-/-}$ and Calu-6 cells, a colon and lung cancer cell line respectively, were incubated with indicated ODNs for 24, 48 and 72 h and cytotoxicity was evaluated by MTT assay. Figure 5 shows that the ODNs of the D-series, still retaining anticoagulant properties (see above) and completely degraded after 24 h in FBS (see below), are characterized by a strong different trend in the two tested cancer cells, in particular they showed the greatest cytotoxicity against Calu-6 cells at all time and concentrations used compared to the results obtained in HCT 116$^{p53-/-}$ (Figure 5, panels A and B). Taking into account the sensitivity of these ODNs to the nucleases we hypothesize that the strong cytotoxicity effect observed in Calu-6 cells is a consequence of accumulation of guanine or guanine based nucleotide in this specific cells. It is in fact known that high concentrations of these molecules have a cell specific cytotoxic effect contributing to their antiproliferative properties, although the molecular mechanism underlying this activity is still under investigation (32,33). Recently, it has been proposed (33) that guanine deaminase (GDA), an essential enzyme in the guanine degradation pathway, has a key role in determining the cellular cytotoxic selectivity of guanine and guanine based nucleotides. This enzyme was found differentially expressed in various human tissues with higher levels in brain, liver, pancreas, kidneys and gastrointestinal tract (34). Cells, with low levels of GDA, treated with guanine based ODNs are unable to efficiently remove excess of guanine or guanine nucleosides and nucleotides with consequent accumulation of them in the cells. Starting from these observations we hypothesized that the diverse behavior of ODNs of the D-series in Calu-6 cells compared to that in HCT 116$^{p53-/-}$ was associated to different levels of GDA in these cells. To test this hypothesis, total RNA was extracted from both cell lines and subjected to RT-qPCR with primers specific for GDA. The results of these experiments strongly support our hypothesis, the mRNA levels of GDA were significantly lower in Calu-6 cells compared to that found in HCT 116$^{p53-/-}$ cells (Supplementary Figure S7). On the light of this result we conclude that the different behavior, of tested ODNs of the D-series, observed in our model of lung and colon cancer cells can be attributed to differences in the expression levels of GDA in these cell lines. In contrast, all ODNs composed mainly by L-nucleotides (L-series), that we have demonstrated to be completely devoid of anticoagulant activity (see above) and stable in FBS (see below), inhibited cell proliferation in a time and dose dependent manner in both cell lines (Figure 5, panels C and D). Among these ODNs, L-TBA-D3 had the greatest effect on the cell growth. Specifically, the treatment of HCT 116$^{p53-/-}$ and Calu-6 cells with L-TBA-D3 is associated to about 50% of cell death already at 10 μM at 72 h. Furthermore, at a higher concentration (50 μM) all ODNs of L-series exhibited a more potent cytotoxic activity in Calu-6 cells compared to HCT 116$^{p53-/-}$. In particular, 72 h after treatment these ODNs caused about 70% of cell death in Calu-6 cells compared to about 50% in HCT 116$^{p53-/-}$ cells. The whole of the data strongly suggest that the cytotoxic activity contributing to the antiproliferative properties of these ODNs, being completely devoid of anticoagulant activity (see above), should not involve neither the thrombin-mediated processes associated to cancer (35,36), neither the described pathway related to the guanine-based products derived from the degradation of G-rich ODNs (33), since they are highly resistant to nucleases (see below). It is impor-

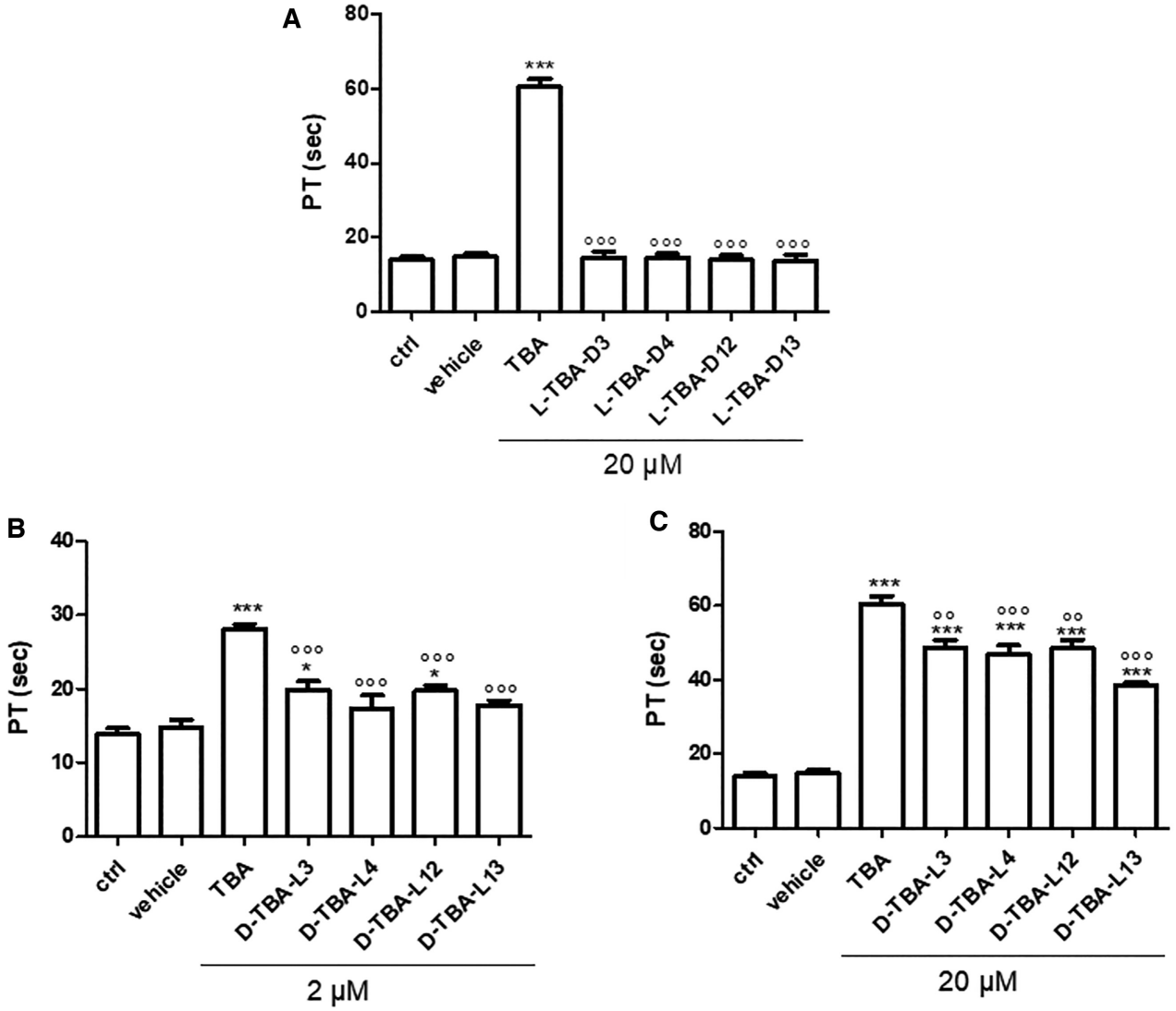

Figure 4. PT values of the enantiomeric TBA derivatives and their natural counterpart at different concentration (2 and 20 μM) with an incubation time of 15 min. See the main text and the Materials and Methods section for details. $^{*}P < 0.05$, $^{***}P < 0.001$ versus vehicle, $^{\circ\circ}P < 0.01$, $^{\circ\circ\circ}P < 0.001$ versus TBA ($n = 3$).

tant to note, that these ODNs are structurally correlated to heterochiral LQ1, previously studied by our group, whose potent cytotoxic activity toward the HCT $116^{p53-/-}$ cells is mediated by a perturbation of nucleolar function with consequent activation of a nucleolar stress response pathway p53 independent and uL3 dependent (21). Further research is needed to verify whether the cytotoxic activity of the investigated ODNs is mediated by the activation of the same molecular pathway.

Nucleases stability

In order to test the resistance in biological environments, all the TBA analogues were undergone to a degradation assay in foetal bovine serum (FBS) and analyzed by circular dichroism (37) (Figure 6 and Supplementary Figure S8). CD spectra of the ODNs composed mainly of L-nucleotides, recorded at 0, 24, 48 and 72 h at 37°C in 10% FBS, were unaffected on changing time, thus indicating a complete resistance of the G-quadruplex structures formed by them. On the contrary, after 24 h ODNs composed mainly of D-nucleotides were completely degraded, as indicated by the absence of G-quadruplex CD signals in the 220–320 nm region, after subtraction of the background scan (10% FBS in DMEM). These data clearly indicate that, as expected, the modified aptamers mostly composed by L-residues, are endowed with an outstanding stability in biological environments.

CONCLUSIONS

In the frame of the research field of the aptamers, TBA represents an unprecedented instance being endowed with two apparently uncorrelated biological activities, namely the anticoagulant and antiproliferative ones. Several investigations showed that suitable modifications in some TBA

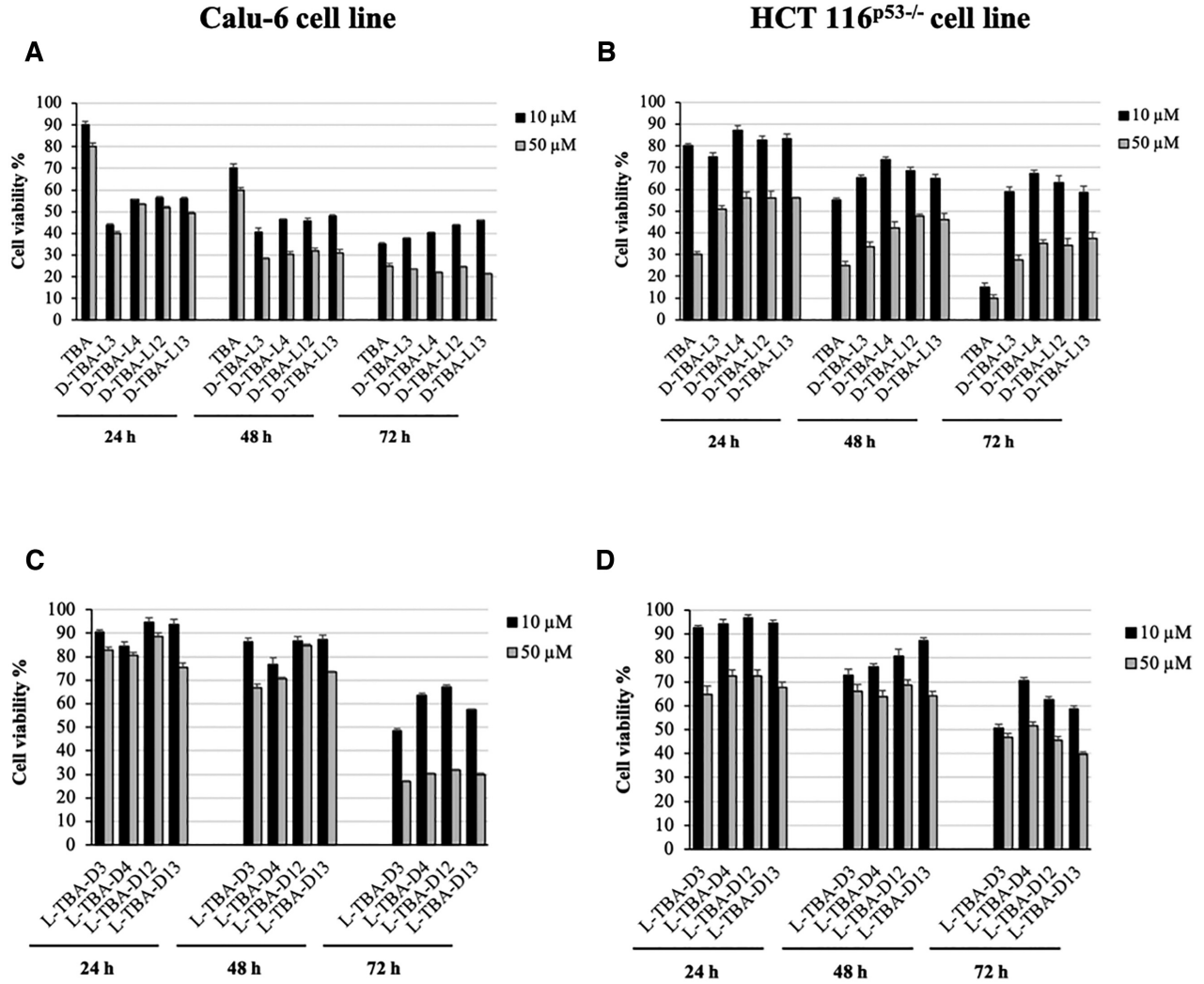

Figure 5. Antiproliferative activity of TBA and its analogues investigated on Calu-6 (panels **A** and **C**) and HCT 116$^{p53-/-}$ (panels **B** and **D**) cell lines. Cells were treated with two different concentrations of indicated ODNs, 10 μM and 50 μM, from 24 to 72 h. Cell viability was assayed using the MTT assay. Results are presented as percentage (mean ± SEM) ($n = 3$) of the untreated cells as control.

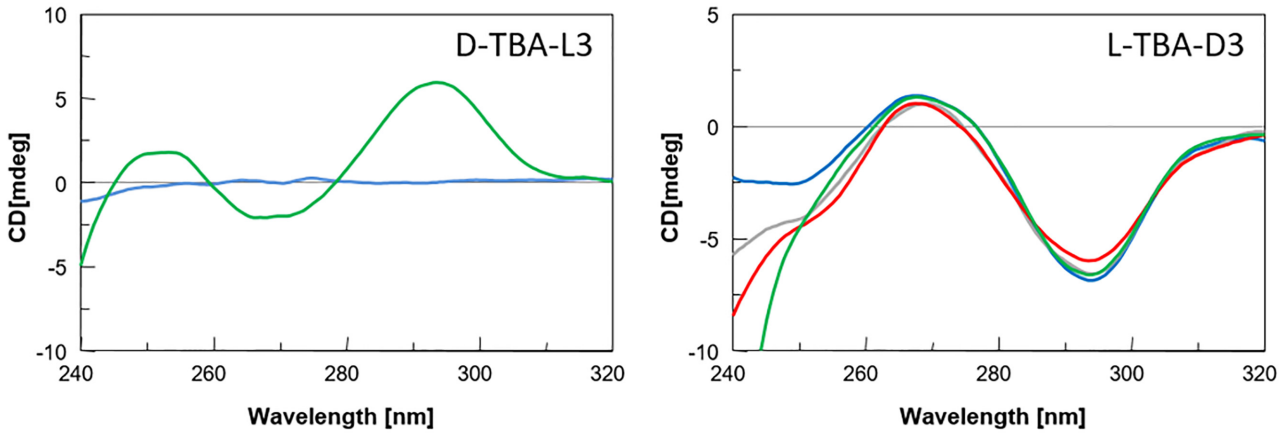

Figure 6. Representative CD spectra of D-TBA-L3 and L-TBA-D3 in 10% fetal bovine serum (FBS) diluted with Dulbecco's modified Eagle's medium (DMEM), registered at 0 (green), 24 (blue), 48 (gray) and 72 h (red), at 37°C. See the main text and the Materials and Methods section for details.

derivatives were able to preserve the antiproliferative activity to the detriment of the anticoagulant one. However, the development as drugs of the antiproliferative TBA derivatives would require a dramatic improvement of their resistance in biological environments compared to the parent TBA. In previous papers, we showed that the use of L-residues in the TBA sequence is a convenient strategy to remove the anticoagulant activity, preserve the antiproliferative one and enhance the resistance to nucleases. Very recently, further investigations suggested that in colon cancer cells the small TT loops of the 'chair-like' G-quadruplex structure play an important role for the antiproliferative activity. In this study, we investigated the structural and biological properties of four couples of enantiomeric heterochiral TBA derivatives each containing a D-residue (L-series) or an L-residue (D-series) in the small TT loops region. All derivatives are able to fold in the 'chair-like' G-quadruplex structure typical of TBA and show noteworthy antiproliferative activities against both colon and lung cancer cells. However, while the TBA derivatives of the D-series preserve the anticoagulant activity in some extent and are completely degraded in biological environment in 24 h, the TBA derivatives of the L-series are devoid of anticoagulant activity and remarkably resistant to nuclease up to 72 h. These results substantiate the potential of the antiproliferative TBA derivatives containing L-residues and open up new perspectives for their utilization against other cancer cell lines. Furthermore, the collected data suggest the participation of biological pathways for the antiproliferative activities independent of the processes involving the guanine-based degradation products or mediated by thrombin. Further TBA derivatives able to take advantage of more than one pathway for the antiproliferative activity have been planned.

SUPPLEMENTARY DATA

Supplementary Data are available at NAR Online.

FUNDING

Regione Campania-POR Campania FESR 2014/2020 'Combattere la resistenza tumorale: piattaforma integrata multidisciplinare per un approccio tecnologico innovativo alle oncoterapie-Campania Oncoterapie' Project [B61G18000470007 to A.R., A.G.]; Fondo di ricerca di base [FFABR-2017 to A.V., V.E., A.R., G.R.]; Ministero della Università e della Ricerca (MIUR). Funding for open access charge: University of Naples Federico II, Department of Pharmacy.

Conflict of interest statement. None declared.

REFERENCES

1. Asamitsu,S., Obata,S., Yu,Z., Bando,T. and Sugiyama,H. (2019) Recent progress of targeted G-quadruplex-preferred ligands toward cancer therapy. *Molecules*, **24**, 429.
2. Carvalho,J., Mergny,J.L., Salgado,G.F., Queiroz,J.A. and Cruz,C. (2020) G-quadruplex, friend or foe: the role of the g-quartet in anticancer strategies. *Trends Mol. Med.*, **26**, 848–861.
3. Roxo,C., Kotkowiak,W. and Pasternak,A. (2019) G-quadruplex-forming aptamers—characteristics, applications, and perspectives. *Molecules*, **24**, 3781.
4. Yazdian-Robati,R., Bayat,P., Oroojalian,F., Zargari,M., Ramezani,M., Taghdisi,S.M. and Abnous,K. (2020) Therapeutic applications of AS1411 aptamer, an update review. *Int. J. Biol. Macromol.*, **155**, 1420–1431.
5. Dapić,V., Abdomerović,V., Marrington,R., Peberdy,J., Rodger,A., Trent,J.O. and Bates,P.J. (2003) Biophysical and biological properties of quadruplex oligodeoxyribonucleotides. *Nucleic Acids Res.*, **31**, 2097–2107.
6. Choi,E.W., Nayak,L. V. and Bates,P.J. (2009) Cancer-selective antiproliferative activity is a general property of some G-rich oligodeoxynucleotides. *Nucleic Acids Res.*, **38**, 1623–1635.
7. Musumeci,D. and Montesarchio,D. (2012) Polyvalent nucleic acid aptamers and modulation of their activity: a focus on the thrombin binding aptamer. *Pharmacol. Ther.*, **136**, 202–215.
8. Avino,A., Fabrega,C., Tintore,M. and Eritja,R. (2012) Thrombin binding aptamer, more than a simple aptamer: chemically modified derivatives and biomedical applications. *Curr. Pharm. Des.*, **18**, 2036–2047.
9. Virgilio,A., Petraccone,L., Vellecco,V., Bucci,M., Varra,M., Irace,C., Santamaria,R., Pepe,A., Mayol,L., Esposito,V. *et al.* (2015) Site-specific replacement of the thymine methyl group by fluorine in thrombin binding aptamer significantly improves structural stability and anticoagulant activity. *Nucleic Acids Res.*, **43**, 10602–10611.
10. Scuotto,M., Rivieccio,E., Varone,A., Corda,D., Bucci,M., Vellecco,V., Cirino,G., Virgilio,A., Esposito,V., Galeone,A. *et al.* (2015) Site specific replacements of a single loop nucleoside with a dibenzyl linker may switch the activity of TBA from anticoagulant to antiproliferative. *Nucleic Acids Res.*, **43**, 7702–7716.
11. Kotkowiak,W., Lisowiec-wachnicka,J., Grynda,J., Kierzek,R., Wengel,J. and Pasternak,A. (2018) Antiproliferative properties of thrombin binding aptamer containing novel UNA derivative. *Mol. Ther. Nucleic Acid*, **10**, 304–316.
12. Virgilio,A., Petraccone,L., Scuotto,M., Vellecco,V., Bucci,M., Mayol,L., Varra,M., Esposito,V. and Galeone,A. (2014) 5-Hydroxymethyl-2′-deoxyuridine residues in the thrombin binding aptamer: Investigating anticoagulant activity by making a tiny chemical modification. *ChemBioChem*, **15**, 2427–2434.
13. Esposito,V., Russo,A., Amato,T., Vellecco,V., Bucci,M., Mayol,L., Russo,G., Virgilio,A. and Galeone,A. (2018) The "Janus face" of the thrombin binding aptamer: Investigating the anticoagulant and antiproliferative properties through straightforward chemical modifications. *Bioorg. Chem.*, **76**, 202–209.
14. Yang,X., Zhu,Y., Wang,C., Guan,Z., Zhang,L. and Yang,Z. (2017) Alkylation of phosphorothioated thrombin binding aptamers improves the selectivity of inhibition of tumor cell proliferation upon anticoagulation. *Biochim. Biophys. Acta - Gen. Subj.*, **1861**, 1864–1869.
15. Esposito,V., Russo,A., Vellecco,V., Bucci,M., Russo,G., Mayol,L., Virgilio,A. and Galeone,A. (2018) Thrombin binding aptamer analogues containing inversion of polarity sites endowed with antiproliferative and anti-motility properties against Calu-6 cells. *Biochim. Biophys. Acta - Gen. Subj.*, **1862**, 2645–2650.
16. Esposito,V., Scuotto,M., Capuozzo,A., Santamaria,R., Varra,M., Mayol,L., Virgilio,A. and Galeone,A. (2014) A straightforward modification in the thrombin binding aptamer improving the stability, affinity to thrombin and nuclease resistance. *Org. Biomol. Chem.*, **12**, 8840–8843.
17. Vater,A. and Klussmann,S. (2015) Turning mirror-image oligonucleotides into drugs: the evolution of Spiegelmer® therapeutics. *Drug Discov. Today*, **20**, 147–155.
18. Virgilio,A., Varra,M., Scuotto,M., Capuozzo,A., Irace,C., Mayol,L., Esposito,V. and Galeone,A. (2014) Expanding the potential of G-quadruplex structures: formation of a heterochiral TBA analogue. *ChemBioChem*, **15**, 652–655.
19. Aviñó,A., Mazzini,S., Fàbrega,C., Peñalver,P., Gargallo,R., Morales,J.C. and Eritja,R. (2017) The effect of L-thymidine, acyclic thymine and 8-bromoguanine on the stability of model G-quadruplex structures. *Biochim. Biophys. Acta - Gen. Subj.*, **1861**, 1205–1212.
20. Esposito,V., Russo,A., Amato,T., Varra,M., Vellecco,V., Bucci,M., Russo,G., Virgilio,A. and Galeone,A. (2017) Backbone modified TBA analogues endowed with antiproliferative activity. *BBA - Gen. Subj.*, **1861**, 1213–1221.
21. Pecoraro,A., Virgilio,A., Esposito,V., Galeone,A., Russo,G. and Russo,A. (2020) UL3 mediated nucleolar stress pathway as a new

mechanism of action of antiproliferative G-quadruplex TBA derivatives in colon cancer cells. *Biomolecules*, **10**, 583.
22. Pecoraro,A., Carotenuto,P., Russo,G. and Russo,A. (2019) Ribosomal protein uL3 targets E2F1 and Cyclin D1 in cancer cell response to nucleolar stress. *Sci. Rep.*, **9**, 15431.
23. Russo,A., Saide,A., Smaldone,S., Faraonio,R. and Russo,G. (2017) Role of uL3 in multidrug resistance in p53-Mutated lung cancer cells. *Int. J. Mol. Sci.*, **18**, 547.
24. Pecoraro,A., Carotenuto,P., Franco,B., De Cegli,R., Russo,G. and Russo,A. (2020) Role of uL3 in the crosstalk between nucleolar stress and autophagy in colon cancer cells. *Int. J. Mol. Sci.*, **21**, 2143.
25. Russo,A., Maiolino,S., Pagliara,V., Ungaro,F., Tatangelo,F., Leone,A., Scalia,G., Budillon,A., Quaglia,F. and Russo,G. (2016) Enhancement of 5-FU sensitivity by the proapoptotic rpL3 gene in p53 null colon cancer cells through combined polymer nanoparticles. *Oncotarget*, **7**, 79670–79687.
26. De Filippis,D., Russo,A., D'Amico,A., Esposito,G., Concetta,P., Cinelli,M., Russo,G. and Iuvone,T. (2008) Cannabinoids reduce granuloma-associated angiogenesis in rats by controlling transcription and expression of mast cell protease-5. *Br. J. Pharmacol.*, **154**, 1672–1679.
27. Russo,G., Cuccurese,M., Monti,G., Russo,A., Amoresano,A., Pucci,P. and Pietropaolo,C. (2005) Ribosomal protein L7a binds RNA through two distinct RNA-binding domains. *Biochem. J.*, **385**, 289–299.
28. De Filippis,D., Russo,A., De Stefano,D., Cipriano,M., Esposito,D., Grassia,G., Carnuccio,R., Russo,G. and Iuvone,T. (2014) Palmitoylethanolamide inhibits rMCP-5 expression by regulating MITF activation in rat chronic granulomatous inflammation. *Eur. J. Pharmacol.*, **725**, 64–69.
29. Yu Wang,K., McCurdy,S., Shea,R.G., Swaminathan,S. and Bolton,P.H. (1993) A DNA aptamer which binds to and inhibits thrombin exhibits a new structural motif for DNA? *Biochemistry*, **32**, 1899–1904.
30. Smith,F.W. and Feigon,J. (1993) Strand orientation in the DNA quadruplex formed from the Oxytricha telomere repeat oligonucleotide d(G4T4G4) in solution. *Biochemistry*, **32**, 8682–8692.
31. Wang,Y. and Patel,D.J. (1993) Solution structure of the human telomeric repeat d[AG3(T2AG3)3] G-tetraplex. *Structure*, **1**, 263–282.
32. Zhang,N., Bing,T., Liu,X., Qi,C., Shen,L., Wang,L. and Shangguan,D. (2015) Cytotoxicity of guanine-based degradation products contributes to the antiproliferative activity of guanine-rich oligonucleotides. *Chem. Sci.*, **6**, 3831–3838.
33. Wang,J., Bing,T., Zhang,N., Shen,L., He,J., Liu,X., Wang,L. and Shangguan,D. (2019) The mechanism of the selective antiproliferation effect of Guanine-Based biomolecules and its compensation. *ACS Chem. Biol.*, **14**, 1164–1173.
34. Yuan,G., Bin,J.C., McKay,D.J. and Snyder,F.F. (1999) Cloning and characterization of human guanine deaminase. *J. Biol. Chem.*, **274**, 8175–8180.
35. Zhou,S., Xiao,W., Pan,X., Zhu,M., Yang,Z., Zhang,F. and Zheng,C. (2014) Thrombin promotes proliferation of human lung fibroblasts via protease activated receptor-1-dependent and NF-κB-independent pathways. *Cell Biol. Int.*, **38**, 747–756.
36. Reddel,C., Tan,C. and Chen,V. (2019) Thrombin generation and cancer: contributors and consequences. *Cancers (Basel).*, **11**, 100.
37. Varada,M., Aher,M., Erande,N., Kumar,V.A. and Fernandes,M. (2020) Methoxymethyl Threofuranosyl Thymidine (4′-MOM-TNA-T) at the T7 position of the thrombin-binding aptamer boosts anticoagulation activity, thermal stability, and nuclease resistance. *ACS Omega*, **5**, 498–506.